A 44–93-μs 250–400-mV 0.18-μm CMOS Starter for DC-Sourced Switched-Inductor Energy Harvesters

Andrés A. Blanco, *Graduate Student Member, IEEE*, Gabriel A. Rincón-Mora, *Fellow, IEEE*

***Abstract*— Although microsystems can replenish batteries and energize modules with ambient energy without having to store much energy on board, on-chip photovoltaic cells and thermoelectric generators generate 50–400 mV, which is usually not sufficiently high to operate transistors. Even though stacking cells is possible, the tradeoff in power is ultimately unfavorable because small transducers output little power. Thankfully, transformers can boost millivolt voltages, but not without a significant toll on space. Motion-propelled MEMS switches can also start a harvester, but only in the presence of vibrations. And although 50–300-mV ring- and LC-oscillating networks can charge batteries, initialization requires 1–15 ms. The prototyped 0.18-μm CMOS oscillating starter presented here draws power from 250–450 mV to charge 100 pF to 0.32–1.55 V in 44–92 μs. In steady state, the cost of the starter to the dc-sourced harvester it supports is only a 1.8% drop in power-conversion efficiency.**

***Index Terms*—Energy harvester, thermoelectric, photovoltaic, dc-sourced, low-voltage starter, switched-inductor dc–dc converter.**

I. Energizing Wireless Microsystems

WIRELESS microsensors network together to add performance-enhancing and energy-saving intelligence to large, remote, and inaccessible places like factories, hospitals, etc. [1]–[2]. Tiny batteries, however, store insufficient energy to sustain over years the sensor, processor, and transmitter that these devices normally incorporate. This is why research is resorting to ambient sources for help. But since small transducers generate little power intermittently, the role of the harvesting source is to replenish the small on-board battery that powers the system, as Fig. 1 illustrates.

Of readily available sources like light, heat, motion, and electromagnetic radiation, sunlight generates the most power at 10–15 mW/cm^3 [3]. And even though artificial lighting and heat output considerably less power at 5–100 μW/cm^3 [3], they are pervasive in consumer applications and mechanical systems. At the millimeter scale, however, photovoltaic (PV) cells produce 300–400 mV and thermoelectric generators (TEGs) output 50–150 mV [4], which are hardly sufficient to operate CMOS transistors. Stacking PV cells is possible, but in the case of CMOS cells and artificial lighting not without a substantial loss in output power [3]. And since microchips only drop 5° to 10° C, on-chip TEGs output less than 150 mV.

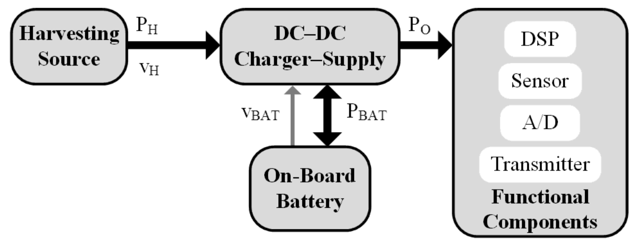

Fig. 1. Wireless microsystem.

With only 50–400 mV at the input and no initial charge in the battery, the conventional charger–supply in Fig. 1 can neither charge the battery nor power the system. This is why Section II of this paper proposes and Section III shows how a prototyped CMOS starter charges a capacitor that supplies start-up energy to the harvester. Section IV then assesses the performance of this technology in light of the applications it supports and the state of the art already reported in literature. Section V ends with a summary of relevant conclusions.

II. Proposed Switched-Inductor Harvester

The self-starting harvesting system first proposed in [5] and now prototyped and shown in Fig. 2 uses a slightly modified starter circuit and a 100-pF capacitor C_{ST} to start the system from no-charge conditions. For this, the starter energizes and drains an inductor L_X in alternating cycles from the input v_H into C_{ST}. When C_{ST} holds enough energy to operate the boost dc–dc converter that the controller and switches S_E and S_B realize, the controller shuts the starter and commands S_E and S_B to transfer input power from v_H to the battery C_{BAT}.

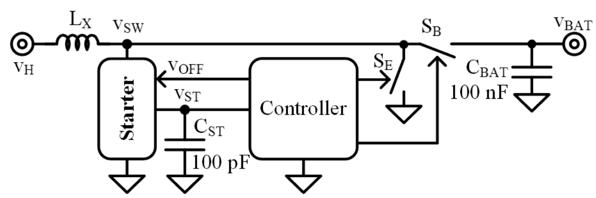

Fig. 2. Proposed self-starting harvester.

A. Oscillating CMOS Starter

L_X and the starter in Fig. 3 comprise an LC oscillator. M_{SEN} is a JFET in [5] and a low-threshold (200 mV) NFET here to remove the need for a JFET. To understand the circuit, consider that, without a harvesting source, all node voltages are 0 V. When v_H first rises above M_{SEN}'s threshold voltage, M_{SEN} conducts and v_H energizes L_X and capacitor C_S across t_E

Manuscript received May X, 2014; revised Month X, 2014; and accepted Month X, 2014. Texas Instruments funded this research.

The authors are with the School of Electrical and Computer Engineering at the Georgia Institute of Technology, Atlanta, GA 30332-0250 U.S.A. (e-mail: ablanco@gatech.edu, Rincon-Mora@gatech.edu).

in Fig. 4. When C_S's v_S rises enough to weaken M_{SEN}'s conduction, L_X's excess current charges parasitic capacitance C_{SW} at switching node v_{SW} until diode-connected and gate-grounded PFETs M_{PD} and M_{P0} conduct to drain L_X into C_{ST}. So across L_X's first de-energizing period t_D, v_{SW} reaches roughly 400 mV and C_{ST}'s v_{ST} begins to rise. v_{ST} continues to rise with every cycle until C_{ST} has enough energy to operate the controller in Fig. 2. At that point, at 38 µs in Fig. 4, when v_{ST} is 0.5 V, the controller raises v_{OFF} to shut the starter.

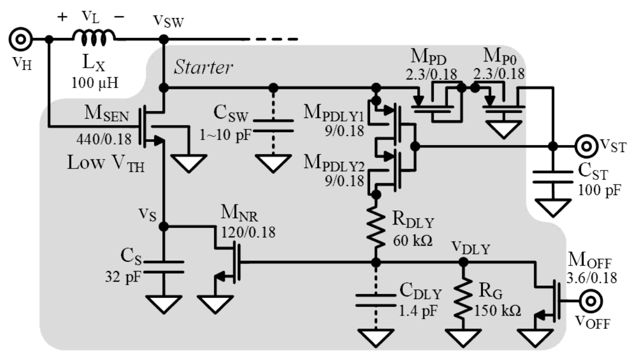

Fig. 3. Prototyped 0.18-µm CMOS oscillating starter.

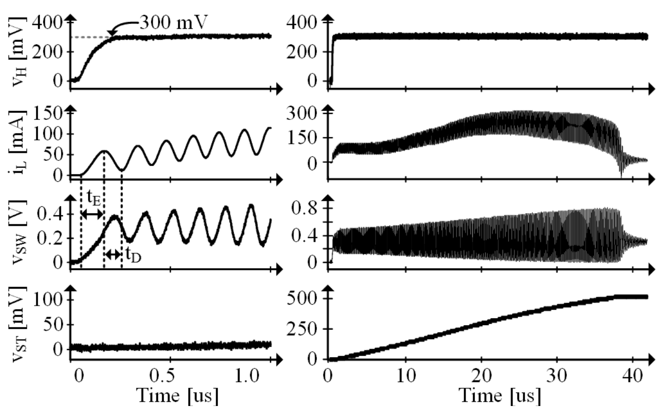

Fig. 4. Measured waveforms of the oscillating starter.

The purpose of M_{PDLY1}, M_{PDLY2}, M_{NR}, R_{DLY}, R_G, and C_{DLY} is to prompt the system to start another energizing sequence. For this, M_{PDLY1} and M_{PDLY2} also draw power from L_X across each de-energizing period t_D, but not to the same extent as M_{PD} and M_{P0} because the impedance across M_{PDLY1}, M_{PDLY2}, R_{DLY}, R_G, and M_{NR}'s parasitic gate capacitance C_{DLY} is higher than that of M_{PD}, M_{P0}, and C_{ST}. Still, C_{DLY} eventually rises and closes M_{NR} after each energizing period t_E to discharge C_S. And with a lower voltage at v_S, M_{SEN} conducts more current to energize L_X and C_S from v_H. Then, as v_S rises across another t_E, M_{SEN} weakens and L_X again drains into C_{SW}, C_{ST}, and C_{DLY} to repeat the sequence. The purpose of R_G in all this is to drain C_{DLY} and open M_{NR} before the end of each energizing period t_E.

M_{SEN}, M_{PDLY1}–M_{PDL2}, R_{DLY}, and M_{NR} enclose a positive feedback loop that oscillates. L_X energizes from v_H when M_{SEN}'s conduction is strong and drains into C_{SW}, C_{ST}, and C_{DLY} when M_{SEN}'s conduction is weak. C_S delays the energizing period and C_{DLY} the drain period to ensure L_X draws and delivers sufficient energy from v_H to C_{ST}. Since M_{SEN}'s resistance is low, v_H energizes L_X, C_S, and C_{SW} in roughly a quarter cycle of L_X, C_S, and C_{SW}'s resonance period:

$$t_E \approx \frac{t_{LC}}{4} = \frac{2\pi}{4}\sqrt{L_X\left(C_S + C_{SW}\right)}\,. \tag{1}$$

Afterwards, L_X partially drains into C_{SW}, and then into C_{ST} and C_{DLY} as long as M_{NR} remains open, that is, as long as C_{DLY} draws current from R_{DLY} and R_G to close M_{NR}.

M_{PDLY1} and M_{PDLY2} (which were one PFET in [5]) are connected in series to keep either body diode from activating when configured to be off. M_{SEN} is a low-threshold NFET because its gate voltage is v_H, which is low. The purpose of M_{P0} and its grounded gate is to set the voltage at v_{SW} above which L_X starts draining into C_{ST}. This way, M_{PD} and M_{P0} do not conduct into C_{ST} until v_{SW} rises above M_{PD}'s and M_{P0}'s two source–gate voltages $2v_{SGP}$. This is important when the startup process begins because C_{ST}'s v_{ST} is zero and M_{PD} without M_{P0} would start draining L_X when v_{SW} reaches v_{SGP}. And since C_{DLY}'s v_{DLY} is a voltage-divided impression of v_{SW}, v_{SGP} at v_{SW} is not high enough to raise v_{DLY} above M_{NR}'s zero-bias threshold V_{TN0}.

B. Design Considerations

<u>*Minimum Gate Drive*</u>: To start energizing L_X, M_{SEN} must conduct current. For this, M_{SEN}'s gate voltage v_H must first surpass M_{SEN}'s threshold voltage $v_{TN(SEN)}$.

$$v_H > v_{TN(SEN)}\,. \tag{2}$$

This is why M_{SEN} is a low-threshold transistor.

<u>*Gate-Drive Degeneration*</u>: To start draining L_X, M_{SEN}'s current i_{SEN} must fall below L_X's built-up current i_L. But since L_X energizes as long as v_H is greater than v_{SW}, i_L does not stop rising until v_{SW} reaches v_H. At this point, i_{SEN} must be lower than i_L for what remains of i_L to charge C_{SW} and raise v_{SW} to the point i_L can also charge C_{ST} and C_{DLY}. For this, i_{SEN} must charge C_S enough for v_S to collapse M_{SEN}'s gate drive. And since M_{SEN}'s bulk terminal is at ground in Fig. 3, raising v_S increases M_{SEN}'s threshold voltage v_{TN}, which means bulk effects further degenerate M_{SEN}'s gate drive. Still, M_{SEN}'s drain–source resistance and C_S's capacitance should be low. But C_S should also be high enough to extend the energizing period t_E to the point L_X draws sufficient energy from v_H to then charge C_{SW}, C_{ST}, and C_{DLY}.

<u>*Minimum Input Energy*</u>: Across each energizing period t_E, M_{SEN} consumes power and C_{SW} and C_S draw energy from v_H. So for L_X to hold energy at the end of t_E, v_H must supply with $E_{H(E)}$ more energy than C_{SW}, C_S, and M_{SEN} require with $E_{SW(E)}$, $E_{S(E)}$, and $E_{SEN(E)}$:

$$E_{H(E)} > E_{SW(E)} + E_{S(E)} + E_{SEN(E)}\,. \tag{3}$$

To finish the first energizing event, v_H must charge C_{SW} from zero to v_H, so $E_{SW1(E)}$ is

$$E_{SW1(E)} = 0.5 C_{SW} v_H^{\ 2}\,. \tag{4}$$

v_H must similarly charge C_S across Δv_S, enough to weaken M_{SEN}'s i_{SEN} below L_X's i_L, so $E_{S(E)}$ is

$$E_{S(E)} = 0.5 C_S \Delta v_S^{\ 2}\,. \tag{5}$$

But to charge C_{SW} to v_H and C_S across Δv_S with q_H, v_H must supply with the first energizing event

$$E_{H1(E)} = q_H v_H = \left(C_{SW} v_H + C_S \Delta v_S\right) v_H\,. \tag{6}$$

In other words, v_H must be high enough for $E_{H(E)}$ to not only charge C_{SW} and C_S but also supply M_{SEN}'s consumption. This is why M_{PD} and M_{P0} are small, to keep C_{SW} and its uncollectable energy low.

Sustaining Oscillations: For oscillations to persist, M_{NR}'s gate voltage v_{DLY} must rise high enough after each energizing period t_E to reset M_{NR} and start another energizing event. Plus, v_{DLY} must reach its target before L_X exhausts its energy because L_X would otherwise stop charging C_{DLY} before M_{NR} can reset. In other words, v_{DLY}'s delay t_{DLY} must be shorter than L_X's exhaust time t_{EX} when drained across v_H and v_{SW}:

$$t_{DLY} < t_{EX} = L_X\left(\frac{\Delta i_L}{\Delta v_L}\right) = L_X\left(\frac{\Delta i_L}{v_{SW} - v_H}\right). \tag{7}$$

For this, L_X first charges C_{SW} across Δv_{SW}, and v_{DLY} then follows after M_{PDLY1} and M_{PDLY2} short and L_X charges C_{DLY} via R_{DLY} and R_G. v_{DLY} therefore reaches 90% of the voltage-divided fraction of v_{SW} that R_{DLY} and R_G set after roughly 2.3 RC time constants t_{RC}:

$$\Delta v_{DLY} \approx v_{SW}\left(\frac{R_G}{R_{DLY} + R_G}\right)\left[1 - e^{-\left(\frac{t_{DLY}}{t_{RC}}\right)}\right], \tag{8}$$

where M_{PDLY1}–M_{PDLY2}'s resistance is much lower than R_{DLY} and t_{RC} is, in consequence, $R_{DLY}||R_G$ and C_{DLY}'s time constant:

$$t_{DLY} \approx 2.3t_{RC} \approx 2.3(R_{DLY} \parallel R_G)C_{DLY}. \tag{9}$$

Since M_{NR} resets the system before v_{DLY} can reach 100% of v_{SW}'s voltage-divided fraction, t_{DLY} is about $2.3t_{RC}$.

When the system first starts, C_{SW} must charge from zero to M_{PD} and M_{P0}'s two source–gate voltages $2v_{SGP}$, so L_X drains when its terminal voltages are roughly v_H and $2v_{SGP}$. v_{DLY} must then rise above M_{NR}'s zero-bias threshold voltage V_{TN0} for M_{NR} to engage. This means, the voltage-divided fraction R_{DLY} and R_G set from v_{SW}'s $2v_{SGP}$ must be greater than V_{TN0}:

$$2v_{SGP}\left(\frac{R_G}{R_{DLY} + R_G}\right) > V_{TN0}, \tag{10}$$

and v_{DLY} must rise above V_{TN0} across t_{DLY} before L_X depletes at t_{EX} when drained with $2v_{SGP} - v_H$.

M_{NR} should then reset M_{SEN} across t_{RES} before R_G discharges C_{DLY} across t_{DIS}:

$$t_{RES} \approx 2.3C_S\left(R_{SEN} \parallel R_{NR}\right) < t_{DIS}, \tag{11}$$

where R_{SEN} and R_{NR} are M_{SEN} and M_{NR}'s resistances and t_{RES} is roughly 2.3 time constants of C_S, R_{SEN}, and R_{NR}. And R_G should drain C_{DLY} before the energizing event ends. So about 2.3 time constants of R_G and C_{DLY} must elapse before t_E:

$$t_{DIS} \approx 2.3R_GC_{DLY} < t_E. \tag{12}$$

III. Measured Performance

The 600 × 250-μm² 0.18-μm CMOS die in Fig. 5b integrates the oscillating starter in Fig. 3, the startup capacitor C_{ST} in Figs. 2–3 and 5a, and the power transistors M_E and M_{B1}–M_{B2} in Fig. 5a. The printed circuit board (PCB) in Fig. 5c embeds the fabricated microchip, the 100-μH inductor L_X in Figs. 2–3 and 5a, the controller in Figs. 2 and 5a, the 100-nF battery C_{BAT} in Figs. 2 and 5a, and test circuits used to evaluate the system. Operationally, the starter charges C_{ST} until C_{ST} stores enough energy for the controller to operate M_E and M_{B1}. Afterwards, M_E energizes L_X from the harvesting source v_H and M_{B1}–M_{B2} drains L_X into C_{BAT} in alternating cycles. The purpose of the diode-connected transistor M_{B2} is to block reverse battery current that would otherwise drain C_{BAT}. Here, the converter that M_E, M_{B1}, M_{B2}, and the controller realize is for test purposes only, to show how the starter affects the dc-sourced harvester it supports.

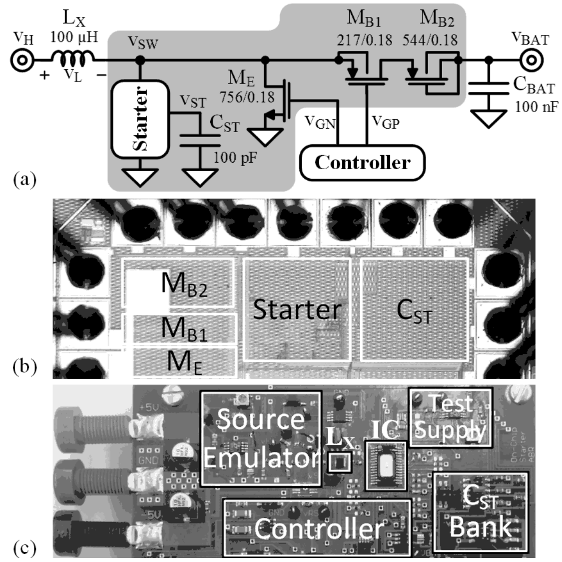

Fig. 5. Prototyped harvesting system, die, and board.

A. Starter

As Fig. 4 demonstrates, the starter energizes and drains L_X in alternating cycles when v_H rises to 300 mV to charge C_{ST} to 500 mV in 38 μs. The system starts as long as v_H ramps to its target within 300 ns, before L_X, C_S, and C_{SW} have a chance to drain with resonance. The oscillator starts without the power-on-reset transistor and signal that [5] needs. Oscillations persist as long as v_H is at or above 255 mV, as Fig. 6 shows.

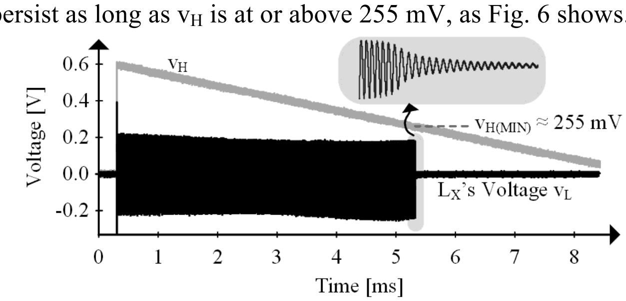

Fig. 6. Measured starter waveforms when C_{ST} is a pre-charged battery.

Notice in Fig. 4 that the system stops charging C_{ST}'s 100 pF at 500 mV. This happens because L_X first energizes more than it drains to build current i_L in L_X, but later drains more than it receives to collapse i_L. So when connected to a drained C_{ST}, 250 and 450 mV at v_H can charge C_{ST} to 320 mV and 1.55 V, respectively, as Fig. 7 shows. This means, the system charges C_{ST}, but only to the extent that v_H allows. This relationship is nearly independent of C_{ST}, as Fig. 8 further shows, with only a ±2.5% variation across 0.1–1.6 nF. So irrespective of the energy needed to charge C_{ST}, the effective gain of the system from v_H to C_{ST}'s final voltage $V_{ST(F)}$ is 1.28–3.47 V/V.

Since $V_{ST(F)}$ depends on v_H, but not on C_{ST}, the startup time t_{ST} that the system requires to charge C_{ST} to $V_{ST(F)}$ climbs with v_H and C_{ST}. This is why t_{ST} in Figs. 9 and 10 spans 44–93 μs for 250–450 mV at v_H and 64–783 μs for 0.1–1.6 nF. Through this time, C_{ST} receives 0.15% to 0.65% of the energy that v_H sources. Power-conversion efficiency across startup is low because the system lacks the gate drive necessary to keep

Ohmic losses low. With lower losses, L_X would have been able to draw and deliver more power.

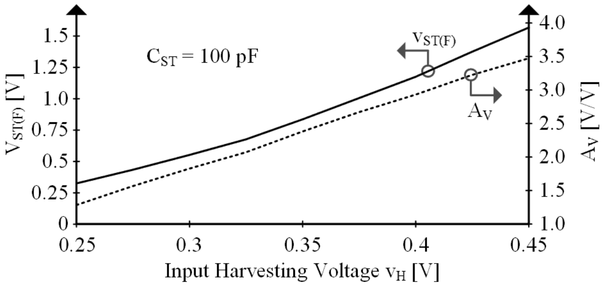

Fig. 7. Measured final startup voltage and gain across v_H.

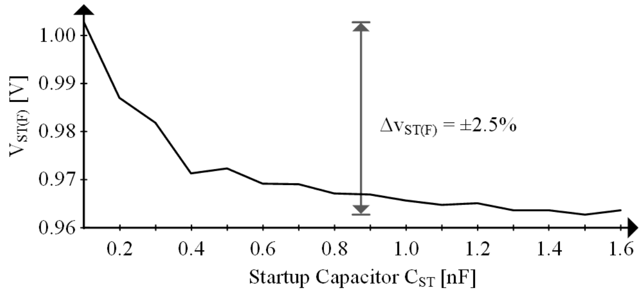

Fig. 8. Measured final startup voltage across C_{ST}.

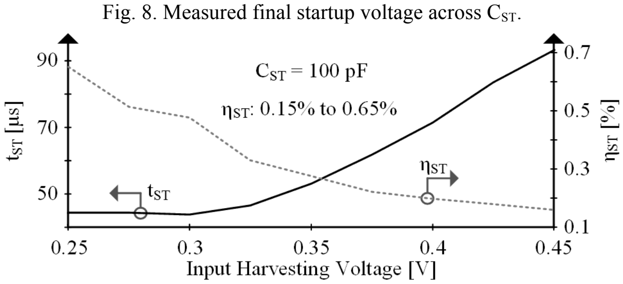

Fig. 9. Measured startup time and conversion efficiency across v_H.

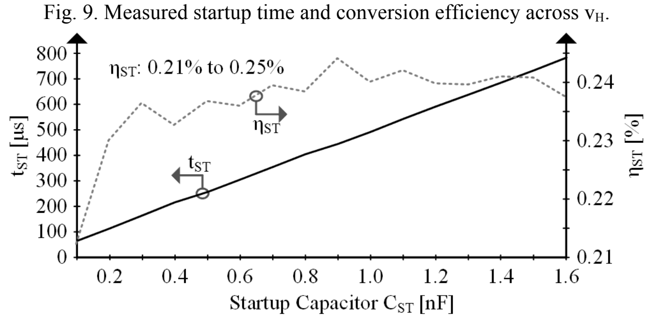

Fig. 10. Measured startup time and conversion efficiency across C_{ST}.

B. Harvesting System

Although C_{ST}'s v_{ST} in Fig. 9 climbs to 830 mV in 53 µs, the controller in Fig. 5a interrupts the startup process with v_{OFF} when v_{ST} surpasses its headroom limit, which in the example of Fig. 5a is 0.7 V, after 41 µs of t_{STRT} in Fig. 11. With 0.7 V across C_{ST}, the controller closes M_E, and as a result, energizes L_X from v_H via a low-resistance switch. This way, L_X draws more energy from v_H, so when M_E opens, M_{PD} and M_{P0} in the starter of Fig. 3 steer L_X's i_L into C_{ST} to raise v_{ST} another 0.3 V after only one cycle, at 46 µs. After that, the controller closes M_E and M_{B1} in alternating cycles to energize and drain L_X into C_{BAT}. So after three cycles at 62.5 kHz in steady state, the voltage across C_{BAT}'s 100 nF rises 210 mV.

Without the starter and in steady state, M_E and M_{B1}–M_{B2} in Fig. 5a charge C_{BAT} with 62% to 74% of the 10–160 µW that the system receives from the harvesting source v_H, as Fig. 12 shows. The cost of connecting the starter is 1.8%. The reason for this loss is the energy lost to charging C_S and the additional capacitance that the starter adds to v_{SW}. For one, C_S partially drains L_X when L_X drains because M_E in Fig. 5a first discharges C_S through M_{SEN} in Fig. 3 when M_E energizes L_X. With C_S's v_S nearly at 0 V, v_H closes M_{SEN} to draw current from L_X and charge C_S. Charging C_{SW} similarly draws power from L_X, which is why adding board capacitance to v_{SW} raises the loss in Fig. 12 to 3.9%. Note that, even after v_{OFF} closes M_{OFF}, M_{PDLY1}, M_{PDLY2}, and R_{DLY} do not dissipate much of L_X's energy because C_{ST}'s v_{ST} keeps M_{PDLY1} and M_{PDLY2} off.

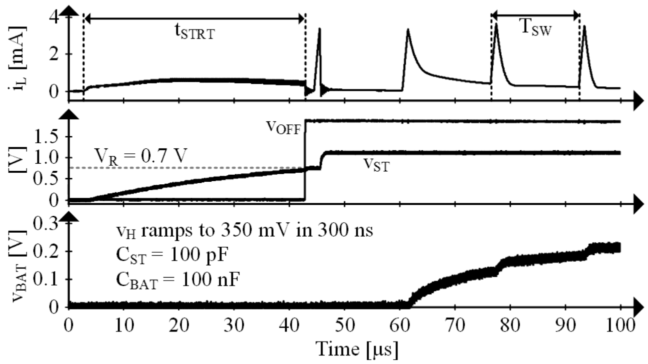

Fig. 11. Measured startup, transition, and steady-state waveforms.

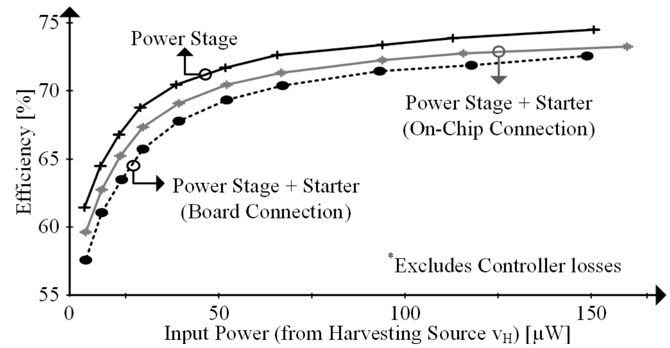

Fig. 12. Measured steady-state power-conversion efficiency.

IV. Context

One fundamental requirement for a microsensor is not to burden its host. This means, it should be small and self-powered. And since tiny photovoltaic cells and thermoelectric generators output little power, conduction, gate-drive, quiescent, and start-related losses should be low, which is why conversion efficiency should be high [6]. But to keep startup losses at bay, startup time should also be short. So in all, the system should be small and efficient, and start quickly.

A. The State of the Art

One way to boost the input voltage to sufficiently high levels to operate CMOS switches is with a transformer [7]–[8]. And with a low-loss transformer, the system can convert and transfer power efficiently in steady state. Unfortunately, a low-loss transformer is, in relative terms, bulky and expensive.

Although transistors powered from 300–400-mV supplies are resistive, they can still steer currents and transfer power. In fact, ring oscillators in [9]–[13] can drive CMOS transistors to switch capacitors that generate a voltage that is high enough to then energize and drain an inductor into a battery. And by tuning N- and P-channel MOS threshold voltages to balance, the network can operate with an 80-mV input [14]–[15], as Table I shows. LC oscillators can similarly operate with a 50-

mV supply [16]. The problem here is that resistances are so high at 50–330 mV and switched capacitors so inefficient that initializing the system requires 1.2–15 ms. Plus, the LC oscillator requires two 4-μH inductors and tuning threshold voltages is prohibitively expensive in practice. Although the prototyped system starts from 250 mV from Fig. 7, v_H in Table I is 300 mV because performance is more comparable to the state of the art when C_{ST}'s final voltage $V_{ST(F)}$ is 0.55 V.

TABLE I
RELATIVE PERFORMANCE

	X-former [8]	Ring Oscillator		LC Osc. [16]	MEMS [4]	This Work
		[12]	Tuned [15]			
$v_{H(MIN)}$	40 mV	330 mV	80 mV	50 mV	35 mV	0.3 V
t_{INI}	–		2.4 ms	15 ms	–	–
t_{ST}	2 s	1.2 s	+500 μs	+100 μs	t_{VIB}	44 μs
$V_{ST(F)}$	1.2 V	1.8 V	1.3 V	0.8 V	1 V	0.55 V
C_{ST}	10 μF		10 nF	4.7 nF	470 pF	100 pF
C_{BAT}				1 μF	100 nF	100 nF
Extra	X-former & 30 pF		132 pF	2× 4 μH	MEMS	32 pF

In [4], motion opens and closes an electromechanical MEMS switch that energizes and drains an inductor into 470 pF until the capacitor's voltage is high enough to drive a CMOS transistor. Since motion drives the MEMS device, the system can start from a 35-mV input. The drawback here is motion, because vibrations are not always available, and when they are, the period is long, so starting the system can require 3–20 ms. Plus, the switching interruptions that motion causes in steady state reduce how much power the system can output.

The benefits of the technology presented here are size, cost, and speed. For the first two, the entire starter can be on chip, and the efficiency sacrificed in steady state for this feature is only 1.8%. And lastly, startup time is within 100 μs. One limitation of this technology is that the harvesting source must rise within 300 ns for the system to start, which is not always possible. The voltage of the input source also limits the starter's final voltage. These restrictions, however, are not necessarily insurmountable, and research is ongoing. Plus, fast start-up applications are emerging, like when office lights or car headlights first shine on a miniaturized photovoltaic cell.

V. CONCLUSIONS

The prototyped 0.18-μm CMOS starter built, tested, and presented here charges 100 pF to 0.32–1.55 V from 250–450-mV sources in 44–93 μs. The starter reduces the steady-state power-conversion efficiency of the harvester it supports by only 1.8%. Although functionality and output voltage depend on the input, 350 mV can still generate 830 mV, which is high enough to operate a CMOS harvester with reasonable efficacy. This is important because tiny photovoltaic cells and thermoelectric generators output only 50–400 mV, which is not enough to drive and energize a wireless microsensor.

ACKNOWLEDGMENT

The authors thank Texas Instruments for sponsoring this research and Paul Emerson for his support.

REFERENCES

[1] R. Vullers, *et al.*, "Energy Harvesting for Autonomouns Wireless Sensor Networks," *IEEE Solid-State Circuits Magazine*, vol. 2, pp. 29–38, 2010.

[2] D. Puccinelli and M. Haenggi, "Wireless Sensor Networks: Applications and Challenges of Ubiquitous Sensing," *IEEE Circuits and Systems Magazine*, vol. 5, pp. 19–31, 2005.

[3] R.D. Prabha and G.A. Rincon-Mora, "CMOS Photovoltaic-cell Layout Configurations for Harvesting Microsystems," *IEEE Int. Midwest Symp. on Circuits and Systems*, pp. 368-371, Aug. 2013.

[4] Y.K. Ramadass and A.P. Chandrakasan, "A Battery-Less Thermoelectric Energy Harvesting Interface Circuit with 35 mV Startup," *IEEE J. of Solid-State Circuits*, vol. 46, pp. 333–341, January 2011.

[5] A.A. Blanco and G.A. Rincon-Mora, "On-chip Starter Circuit for Switched-inductor DC-DC Harvester Systems," *IEEE Int. Circuits and Systems Symp.*, pp. 2723–2726, May 2013.

[6] R.D. Prabha and G.A. Rincon-Mora, "Harvesting Circuits for Miniaturized Photovoltaic Cells," *IEEE Int. Circuits and Systems Symp.*, pp. 309-312, May 2011.

[7] Linear Technology, LTC3108 Datasheet, 2010.

[8] J. Im, *et al.*, "A 40mV Transformer-reuse Self-startup Boost Converter with MPPT Control for Thermoelectric Energy Harvesting," *IEEE J. of Solid-State Circuits*, vol. 47, pp. 3055–3067, Dec 2012.

[9] G. Schrom, *et al.*, "On the Lower Bounds of CMOS Supply Voltage," *Solid-State Electronics*, vol. 39, pp. 425–430, April 1996.

[10] T. Niiyama, *et al.*, "Dependence of Minimum Operating Votlage (V_{DDmin}) on Block Size of 90-nm CMOS Ring Oscillators and Its Implications in Low Power DFM," *9th Int. Symposium on Quality Electronic Design*, pp. 133–136, March 2008.

[11] N. Sze, W. Ki, and C. Tsui, "Threshold Voltage Start-up Boost Converter for Sub-mA Applications," *4th IEEE Int. Symp. on Electronic Design, Test & Applications*, pp. 338–341, Jan. 2008.

[12] K. Kadirvel, *et al.*, "A 330nA Energy-harvesting Charger with Battery Management for Solar and Thermoelectric Energy Harvesting," *IEEE Int. Solid-State Circuits Conf.*, pp. 106–107, Feb. 2012.

[13] A. Richelli, S. Comensoli, and Z.M. Kovacs-Vajna, "A DC/DC Boosting Technique and Power Management for Ultralow-Voltage Energy Harvesting Applications," *IEEE Trans. on Industrial Electronics*, vol. 59, pp. 2701–2708, June 2012.

[14] P. Chen, *et al.*, "Startup Techniques for 95 mV Step-Up Converter by Capacitor Pass-On Scheme and V_{TH}-tuned Oscillator with Fixed Charge Programming," *IEEE J. of Solid-State Circuits*, vol. 47, pp. 1252–1260, May 2012.

[15] P. Chen, *et al.*, "An 80 mV Startup Dual-Mode Boost Converter by Charge-Pumped Pulse Generator and Threshold Voltage Tuned Oscillator with Hot Carrier Injection," *IEEE J. of Solid-State Circuits*, vol. 47, pp. 2554–2562, Nov 2012.

[16] P. Weng, *et al.*, "50 mV-Input Batteryless Boost Converter for Thermal Energy Harvesting," *IEEE J. of Solid-State Circuits*, vol. 48, pp. 1031–1041, April 2013.